PROCEEDINGS, 49th Workshop on Geothermal Reservoir Engineering
Stanford University, Stanford, California, February 12-14, 2024
SGP-TR-227

Measurements of Thermo-Hydro-Mechanical-Chemical Coupling in Granite Shear Fractures at FORGE using the Triaxial Direct-Shear Test Method

Uwaila C. Iyare[1], Luke P. Frash[1], Bijay KC[1], Meng Meng[1], Kayla Kroll[2], Megan M. Smith[2], Gabriela Davila[2], Wenfeng Li[1], Yerkezhan Madenova[1], Oana Marina[1] and James W. Carey[1]

[1]Los Alamos National Laboratory, PO Box 1663, Los Alamos, NM, 87545

[2]Lawrence Livermore National Laboratory, 7000 East Ave, Livermore, CA 94550

uwaila_iyare@lanl.gov

Keywords: Enhanced Geothermal Systems; Triaxial direct-shear test; Fracture Aperture; Permeability; Shear Strength; Granite, FORGE

ABSTRACT

Enhanced Geothermal Systems (EGS) require cold fluid injection as part of the process to extract heat from fractured hot rock to produce electricity. Over time, this cold fluid injection will induce pressure and temperature changes in the fractured rock which will, in-turn, have a feedback effect on fracture permeability through complex thermo-hydro-mechanical-chemical (THMC) coupling. Our study presents lab measurements that characterize shear fractures in granite from the Frontier Observatory for Research in Geothermal Energy (FORGE) site at its in-situ temperature, stress, pressure, and chemical conditions. Using the triaxial direct-shear method, we performed mechanical shearing and flow-through experiments on initially intact (i.e., unfractured) core samples. Applied reservoir conditions were 36.1 MPa total normal stress, 22.2 MPa pore pressure, and temperatures between 180 and 210 °C. Injected fluid was so-called "golf course water" to mimic the tap water chemistry that is being used at FORGE. Measurements included intact shear strength, residual shear strength, intact rock permeability, shear fracture hydraulic aperture, fracture dilation during shearing, stress-dependent fracture aperture, permeability change with temperature, and effluent chemistry changes. When sheared, fractured permeability exhibited a significant increase, often by a factor of 105 or more, and this enhancement was sustained over time. However, shear slip after the initial fracture event did not generate the expected rise in fracture permeability that is typical for room-temperature tests. Permeability then experienced a reduction by a factor of 102 due to stress-induced closure as the confining pressure was raised from 36.1 MPa to 48 MPa, and a similar magnitude reduction was again observed during cooling. Other key observations from our results include a strong tendency for silicate dissolution and magnesium salt precipitation during sustained flow. The shear-dilation was unusually low at 4° ±1° for the high-temperature conditions compared to values of 11° ±5° for room temperature tests. This low dilation coincides with smooth shear fracture surfaces that resembled slickensides and felt waxy to the touch. To the best of our knowledge, our measurements are the first-ever THMC measurements for rock fractures at EGS conditions. These experiments indicate that shear stimulation is unlikely to be effective at FORGE for geothermal reservoir flow enhancement. The experiments also indicate that mineral dissolution and precipitation will be highly active at FORGE conditions with injection water contaminants such as magnesium being key reactants for infilling precipitation in the fractures.

1. INTRODUCTION

Several studies have emphasized the potential of Enhanced Geothermal Systems (EGS) as a viable energy source for electricity production in the United States, offering the possibility to bring low-cost geothermal energy to locations that lack natural permeability (Augustine, 2016; Sanyal and Butler, 2005; Tester et al., 2007). Enhancing permeability and establishing EGS reservoirs can be achieved using hydraulic stimulations. Despite global efforts to develop EGS since the late 1970s, no commercially viable EGS reservoirs have been established to date. A key technical challenge to overcome for EGS to become both technically and economically feasible involves comprehending the subsurface mechanisms that influence reservoir creation (through hydro shearing and hydraulic fracturing stimulation methods) and long-term sustainability.

The US Department of Energy (DOE) initiated the Frontier Observatory for Research in Geothermal Energy (FORGE) program to drive research and development for EGS through a dedicated field site (Mckittrick et al., 2019). This effort is part of an initiative to conduct research focusing on the management, control, and sustainability of fractures essential for the flow of a fluid to extract heat from EGS reservoirs. In 2018, the DOE selected a site in south-central Utah for the FORGE program (Figure 1) and this site was selected to provide a controlled environment where technologies for characterizing, creating, and sustaining EGS reservoirs can be developed and tested (Moore et al., 2019; Allis et al., 2016). This study utilizes the data from well drilled in the Utah FORGE site for which cores, wireline logs, seismic data and geological data are available.

A primary objective of the FORGE project is to gather experimental data aiming to deepen our understanding of the subsurface mechanisms that impact the longevity of EGS reservoirs. EGS development entail extracting heat from deep-seated hot rock formations, requiring either existing fractures or induced fractures, along with the injection of fluids into these rocks. The efficiency of heat extraction in EGS is contingent upon maintaining permeability and ensuring adequate fluid movement within these fractures. The ongoing fluid injection, coupled with variations in stress from temperature and pressure fluctuations, brings about alterations in permeability. These changes are influenced by a combination of thermal, hydrological, mechanical, and chemical (THMC) processes. Importantly, it's challenging to isolate the distinct impacts of these THMC processes on permeability changes, as each interacts with the system in ways that can collectively result in either opening or closure of the fracture.

The permeability of fractures can change rapidly due to various factors such as changes in normal stress, pore fluid pressure (Vogler et al., 2018) temperature (Morrow et al., 2001), and chemical equilibrium (Yasuhara et al., 2004). In natural hydrothermal systems, fractures have been observed to undergo cycles of opening and closing due to stress-induced dilation, mineral deposition, brecciation, and localized dissolution and precipitation (Davatzes and Hickman, 2009; Dobson et al., 2021; Huo and Benson, 2016). Such changes in fracture behaviour can significantly impact the hydraulic dynamics of EGS reservoirs, potentially compromising the sustained circulation of fluids in EGS reservoir. In this scenario, coupled THMC effects might cause a decline in heat extraction which thus reduce energy production and make EGS less technically and economically viable option. Understanding these coupled THMC processes is still limited but is crucial for predicting the long-term changes in reservoir permeability associated with geothermal energy extraction (Lima et al., 2019; Pandey & Vishal, 2017).

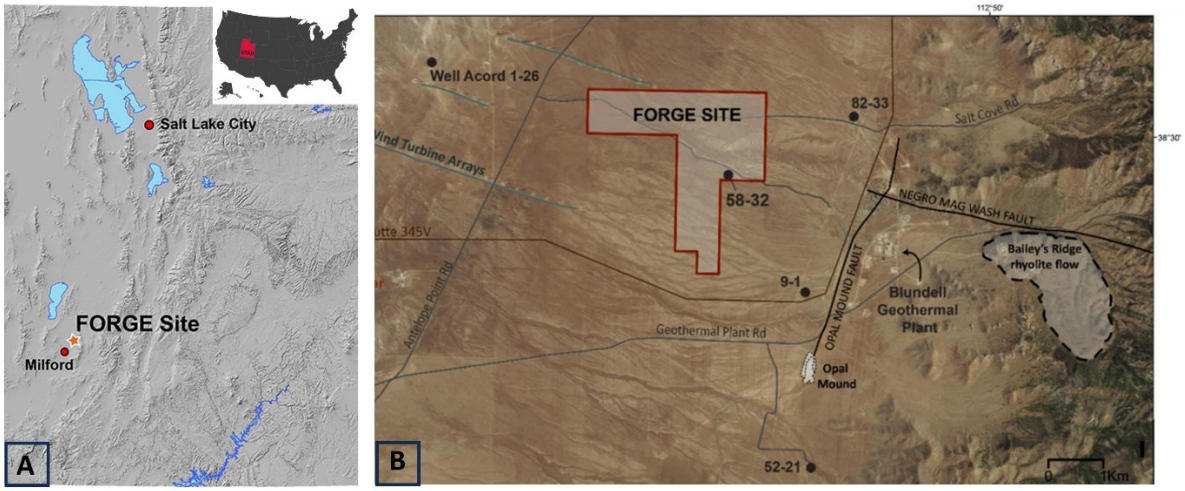

Figure 1: Map showing the Utah FORGE site and its surroundings. The town of Milford is at the center, 16 km south of FORGE. B) Map indicating the FORGE site, key wells, and energy projects, with the Blundell power plant and production wells located east of the Opal Mound fault. Modified from Moore et al., (2019)

The objective of this study is to measure and assess the mechanical, permeability, and chemical changes in shear fractures through a series of core-flooding experiments under pressure and temperature conditions relevant to EGS. To achieve our objective, we employed a triaxial direct-shear (TDS) method. The TDS method enabled us to perform mechanical shearing and flow-through experiments on 1.5-inch diameter FORGE core samples sourced from the Utah FORGE site (FORGE 58-32). These experiments were conducted using the triaxial direct-shear apparatus located at Los Alamos National Laboratory (LANL). By employing this method, we were able to faithfully replicate actual site conditions, including reservoir temperature, shear-oriented in-situ stresses, influent chemistry, and crucially, mechanically induce fractures under in-situ conditions. This approach not only provides highly relevant data but also minimizes the number of experiments required, preserving the valuable core material obtained from the site. Results from these experiments provide: permeability, shear strength, shear fracture hydraulic aperture, fracture dilation during shearing, stress-dependent fracture aperture. These innovative experiments directly pertain to the long-term sustainability of EGS applications. This approach allowed for the simultaneous evaluation of the thermal, hydraulic, mechanical, and chemical (THMC) behaviour of shear fractures formed under EGS-reservoir conditions.

2. GEOLOGICAL SETTING

The geological site for the FORGE project is located on the eastern edge of the Milford basin, west of the Mineral Mountains, Utah (Figure 1). The Mineral Mountains are primarily characterized by a Tertiary-age composite pluton that consists of diorite, granodiorite, quartz monzonite, syenite, and granite, as noted by Nielson et al. (1986). Deep wells drilled nearby have verified the presence of granite and gneiss near the surface, temperatures ranging between 175–225°C, and limited permeability at depths of 2 to 4 km, indicating that the FORGE site is not part of any active hydrothermal system (Allis et al., 2016).

As part of the FORGE program, three new vertical wells have been drilled to date. The deepest is Well 58-32 which was drilled at a depth of 2,297 meters (7,536 feet) to examine the reservoir rocks and thermal conditions. The well encountered mainly granite and quartz monzonite plutonic rocks, with a bottom hole temperature of 199°C, suggesting a conductive thermal environment (Jones et al., 2018; Allis et al., 2016). The stress gradients in the well were determined to be 14 MPa/Km for the minimum principal stress and 17.4 MPa/Km for the maximum principal stress (Moore et al., 2019). Additionally, an overburden stress gradient of 25.6 MPa/Km was calculated. The orientation of the maximum principal stress at the FORGE site, inferred from the Well 58-32 Formation MicroImager (FMI) log, trends NNE-SSW, as evidenced by the azimuths of the induced fractures. Although estimates of in-situ stress are continually updated (Xing et al., 2020), for the purposes of this study, we consider 63.4, 32.5, and 22.0 MPa as maximum total stress, minimum stress, and pore pressure, respectively, for the 2350 m deep site. Assuming a slip angle of 20° with respect to the maximum stress, we derive a 36.1 MPa normal stress, which serves as a reasonable confining pressure for experiments.

3. EXPERIMENTAL MATERIALS AND METHOD

3.1 Rock Sample Description and Preparation

Two granite rock samples from Well 58-32 were used for the experiments (Figure 2), each prepared as precision right-regular cylinder core plugs (labelled as FS04-01 and FS07-01) according to the specifications outlined in D4543-08 (2008). The dimensions of the rock specimens were nominally 1.5 inches in diameter and 1.5 inches in length. The rock's mineralogy comprises quartz, microcline, and Albite. Efforts were made to precisely identify and sub-core weak planes, including natural fractures and foliation parallel to and along the diametric cross-section of the rock specimens, to ensure suitability for mechanical and hydraulic characterization. FS04-01 appears have strong foliation compared to FS07-01. The rock specimens were preserved under room conditions without undergoing drying or saturation steps, as the material had low porosity.

Figure 2: Subset of the Granite rock sample from Utah FORGE site, each with a diameter and length of 1.5 inches, cored to align foliation parallel to the direct shear plane for hydraulic and geomechanical characterization.

3.2 Experimental Apparatus and Procedure

All experiments were conducted using a triaxial direct shear (TDS) system installed at the Fractured earth Laboratory, Los Alamos national Laboratory. The TDS system was designed to fracture the rock specimens under elevated confining stress conditions, while simultaneously measuring permeability of rocks under increasing stress up to and beyond mechanical failure. The TDS apparatus, schematically shown in Figure 3, was initially designed by Carey et al. (2015) and subsequently modified by Frash et al. (2017); Frash et al. (2016); Frash et al. (2019b). This apparatus has a capacity to apply radial confining stresses of up to 70 MPa, and operates at temperature up to 250°C. The triaxial cell employs a 'quad-port' design, featuring one flow line at each end of the sample and two static lines for precise upstream and downstream pressure measurements. The apparatus operates through a stainless-steel body vessel and utilizes silicone oil as a confining medium, with the option for injecting liquid or gas as the pore fluid. In this study, a nearby "golf course water" was used as pore fluid. This water included the contaminant of magnesium, which will later be shown to be important for inducing precipitation during flow.

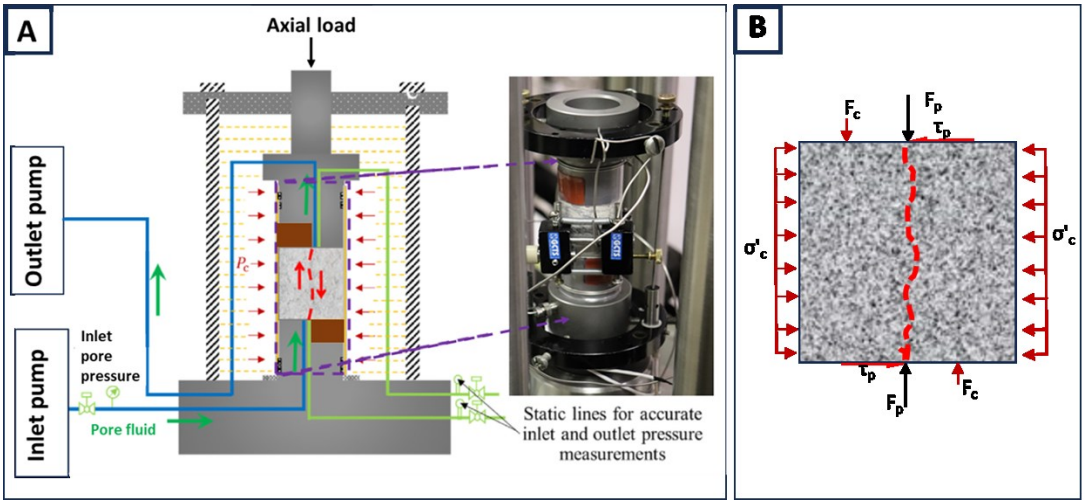

Figure 3: Schematics for the Triaxial direct-shear assembly a) The sample is aligned parallel with the direct-shear plane imposed by the two opposing platens. b) Shear stress distribution in the sample (where F_P is the Axial force and F_c is the force associated with the confining stress). Modified from Meng et al., (2021) and Li et al., (2023)

A distinctive feature of the TDS apparatus involves utilizing opposing L-shaped stainless-steel platens, complemented by silicon rubber fillers, to induce shear fractures along the axial direction of a cylindrical core specimen, enabling stress-dependent measurements of fracture permeability (Li et al., 2023; Li et al., 2021). Figure 4 illustrates the arrangement of the rock specimen in relation to the platens. The specimen is, positioned between the two opposing L-shaped stainless-steel platens which is complemented by silicon rubber fillers and then encased in a Viton flexible tube sleeve, designed to endure temperatures over 200°C. The sleeve serves the dual purpose of isolating pore fluids, from the surrounding silicon oil in the vessel. As the rock specimen is set onto the platens, it is aligned axially, ensuring that its potential weak planes match the shear plane created by the opposing L-shaped platens. To ensure uniform access of pore fluid across the entire specimen end surface, permeable mesh screens are strategically positioned at both ends of the rock specimen (see Figure 4). The 'quad-port' design of the system provides redundant flow and pressure data, contributing to uncertainty quantification in the permeability measurements. Additionally, wire tourniquets secure the ends of the Viton flexible tube sleeve, providing additional reinforcement.

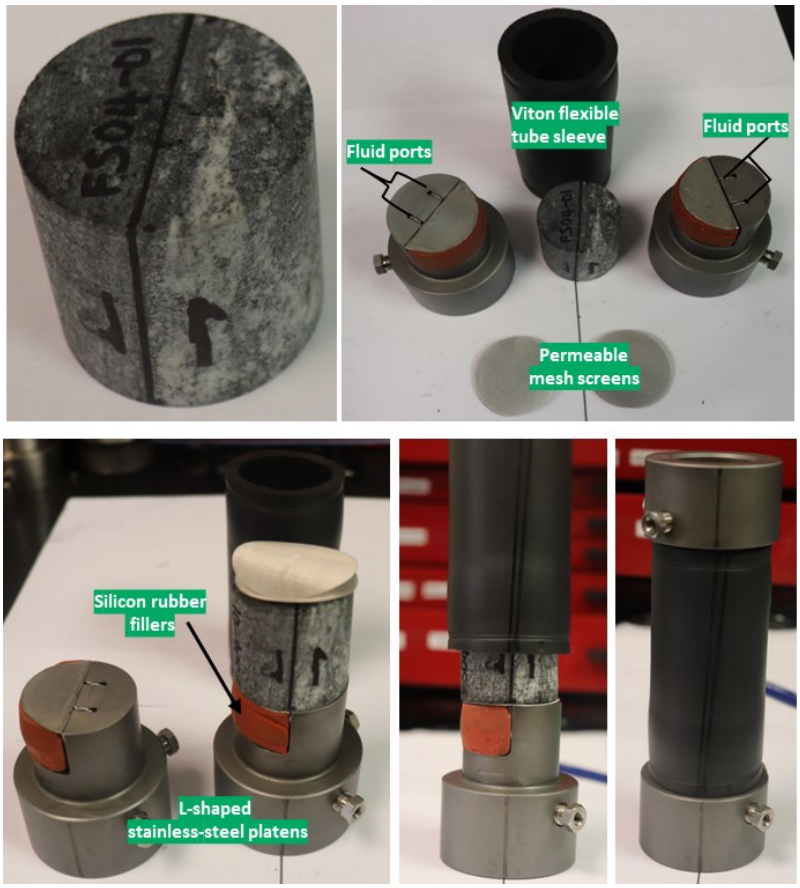

Figure 4: Arrangement of the rock specimen with respect to the platens. The specimen is placed between two opposing L-shaped stainless-steel platens, accompanied by silicon rubber fillers, and enclosed in a Viton flexible tube sleeve designed to withstand temperatures exceeding 200°C. The 'quad-port' design, incorporating two fluid ports at each end of the sample, enables the recording of redundant flow and pressure data, facilitating the quantification of uncertainties in permeability measurements.

The TDS apparatus is designed for the specimens to be loaded in the axial direction by a piston and confined in the pressure vessel using silicone fluid. External pressure from the confining fluid is applied outside the Viton flexible tube sleeve to compress the specimen across its outer radius (σ_c) and on half of each end of the specimen (F_c). Axial force, generated through two opposing L-shaped stainless-steel platens (F_p), induces direct-shear stress in the specimen. Shear fractures along the axial direction of the specimen, are created to facilitate hydraulic conductivity measurement (i.e., permeability). During the tests, the average axial displacement of the rock sample is measured by two linear variable differential transformer (LVDT) position sensors. Additionally, a radial chain device equipped with another LVDT, is used to capture transverse displacement. Teledyne ISCO syringe pumps are used as inlet and outlet pumps and to measure the related flow parameters such as pressure, flow rate, and pump volume. Real-time monitoring captures shear fracturing events often reflected as peak points in the shear stress curve. After shear fracture initiation, additional shear displacements can be applied to evaluate fracture permeability at different shear displacements (Welch et al., 2021).

3.2.1 Experiment procedure

The experimental procedures for the TDS test are summarized as follows:

1. The triaxial vessel was heated to a target temperature close to 200°C.
2. Isotropic confining stress was applied to a target of 36.1 MPa, and the inlet pore pressure was increased to 22.0 MPa, while the outlet pore pressure was increased to 21.0 MPa.
3. Pre-fracture permeability measurement was performed for approximately 10 minutes.
4. Direct shear stress was applied to induce fracturing by increasing axial piston displacement while maintaining constant confining stress. This allowed for an increase in shear displacement at a constant confining stress.
5. Shearing was allowed for axial displacement of 0.0 – 0.5 mm with at least 10 minutes of permeability measurement.
6. Step 5 was repeated for axial displacements of 0.5 – 1.0 mm, 1.0 – 1.5 mm, and 1.5 – 2.0 mm, and permeability measurement was conducted after each displacement interval.
7. Effluent samples were collected after each stepwise event to relate deformation and stress to chemical activity.
8. An additional step of stress cycling with confining stress (36.1 MPa — 24 MPa — 48 MPa — 36.1 MPa) was performed to observe changes in hydraulic aperture as a function of effective confining stress.
9. Additional mechanical shear steps were conducted by changing confining stress downward to establish the Mohr-Coulomb slip criteria for the fractured specimen.
10. The system was unloaded and cooled to ambient laboratory conditions.

3.2.2 Permeability and aperture measurements

In this report, we provide information on both the permeability and fracture aperture. The bulk permeability of the specimen was computed using Darcy's law, as expressed in equation 1 ((Frash et al., 2017):

$$k_{specimen} = \frac{Q\mu L}{\frac{\pi D^2}{4}\Delta p} \quad (1)$$

where Q represents the volumetric flow rate, ΔP is the pressure drop across the specimen, L is the length of the specimen, D is the diameter of the specimen and μ is the dynamic viscosity at 0.14 for water at 200°C. Permeability can be determined with a single flow rate measurement, but for increased accuracy, we calculate permeability by considering redundant flow rates from both the inlet and outlet pumps. This approach enables us to provide an uncertainty estimate. The typical range of our permeability measurements is 1 μD to 100 mD. While the granite matrix exhibits minimal to no permeability, the permeability measured in this study is predominantly influenced by fractures. Consequently, $k_{specimen}$ can be regarded as the permeability of the fracture when the flow area is replaced by the cross-sectional area of the fracture. Hence, the fracture permeability value is contingent upon the geometry employed to delineate the flow path.

For the aperture measurement, we measured hydraulic (b_h) and mechanical (b_d), aperture in our experiments. The mechanical aperture (b_d) was measured using the radial LVDT. The measured values represent the displacement of both the fracture surface and the adjoining rock matrix. We defined the b_h as effective hydraulic opening enabling fluid passage and compute using a parallel-plate approximation based on the cubic law and the assumption of laminar flow through a fracture (Milsch et al., 2016; Witherspoon et al., 1980; Zimmerman and Bodvarsson, 1996) which is given by:

$$b_h = \sqrt[3]{\frac{12Q\mu L}{-\Delta P D}} \quad (2)$$

This equation is related to the specimen bulk permeability $k_{specimen}$ via the following relationships:

$$b_h = \sqrt[3]{3\pi D k_{specimen}} \quad (3)$$

We find that the hydraulic aperture serves as a valuable measure for representing the fluid conductivity of a fracture. This is attributed to its direct scalability to fractures of varying length and width, and its insensitivity to the cross-sectional geometry of the specimen.

3.2.3 Shear strength measurement

The mean direct-shear stresses (τ_{DS}) applied to the specimen is calculated using the following relationship (Frash et al., 2019a) with reference to Figure 3

$$\tau_{DS} = \frac{F_p - F_c}{DL} - \sigma_s \quad (4)$$

Where L is the length of the specimen, D is the diameter of the specimen and σ_s is a calibration value 2 ± 0.9 MPa from tests conducted on split specimens of greased Teflon with a friction coefficient of less than 0.04. The calibration lumps uncertainty from system friction, rubber compression, and other effects into a single term.

4 RESULTS AND ANALYSIS

TDS tests were conducted on two granite rock samples, namely FS07-01 and FS04-01, and each with an approximate diameter and length of 1.5 inches. The results provide insights into the geomechanical and hydraulic behaviour of these samples under triaxial direct-shear conditions at in-situ stress and temperature. The experiments were carried out as a function of shear displacement (δ), effective confining pressure (σ_{eff}) and time. In the TDS tests, the matrix permeability of the intact rock sample is initially assessed before inducing shear fractures parallel to the sample axis under an effective confining stress of 14.1 MPa. Detailed test conditions are depicted in Figure 5.

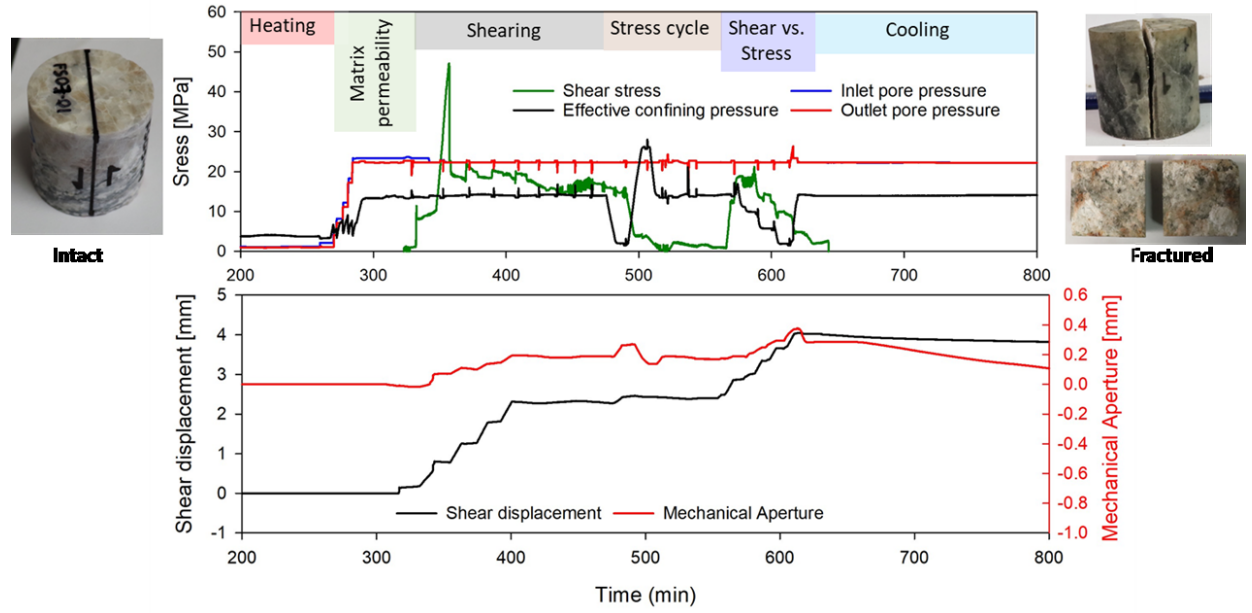

(a) FS07-01

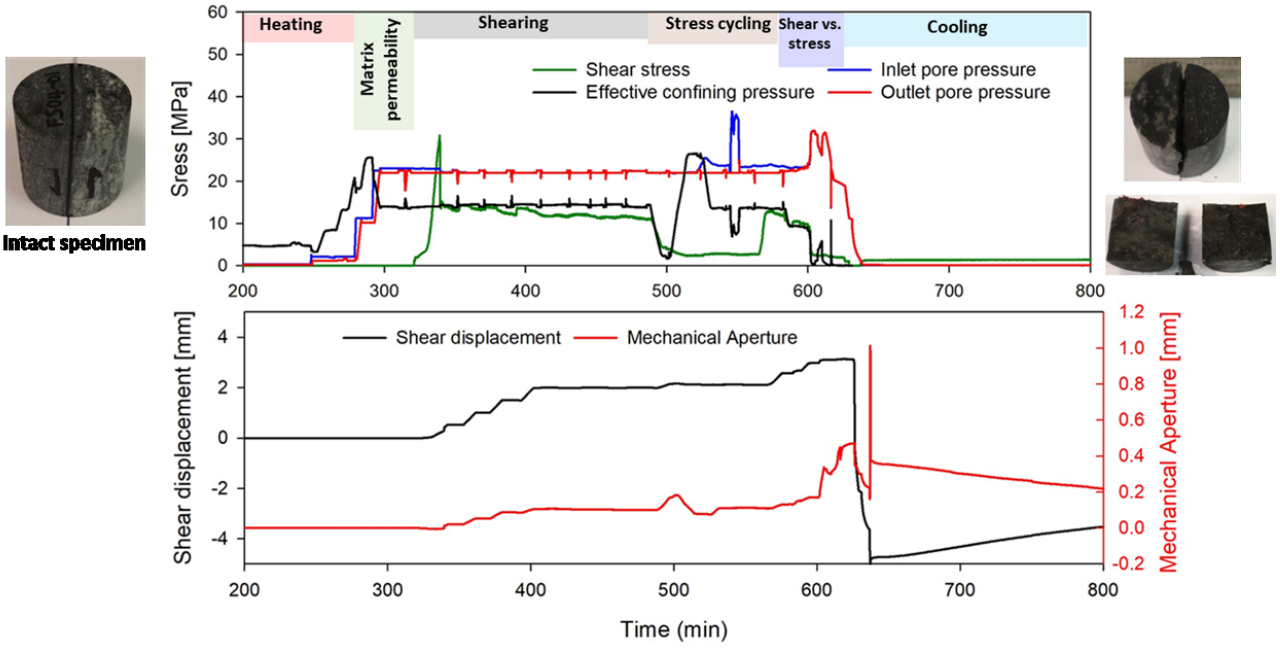

(b) FS04-01

Figure 5: Post-test image and timeseries data obtained for (a) FS07-01sample and (a) FS04-01sample. The upper panels show the applied stress state, effective pressure, inlet, and outlet pore pressures as a function of time and the lower panels show the shear displacement and the mechanical aperture. Effluent sample collection coincides with pore pressure blips during pump disconnections and reconnections.

The topography of the two fractured core surfaces for each sample was carefully examined using an optical surface profilometer. Figure 6 presents both the fractured core surfaces of the rock samples and the corresponding surface profilometry data. Analysis of these surfaces through surface profilometry can offer valuable data for estimating the Joint Roughness Coefficient (JRC). By scrutinizing the profiles of the fractured surfaces, essential information about their roughness characteristics, including amplitude and wavelength of surface irregularities, can be extracted. It is important to note that, as of the preparation of this report, the surface profilometry analysis has not been concluded. Nonetheless, upon physical examination, the sheared fracture surfaces, where the two fractured core surfaces met, appeared smooth, resembling slickensides, and exhibited a waxy texture upon touch.

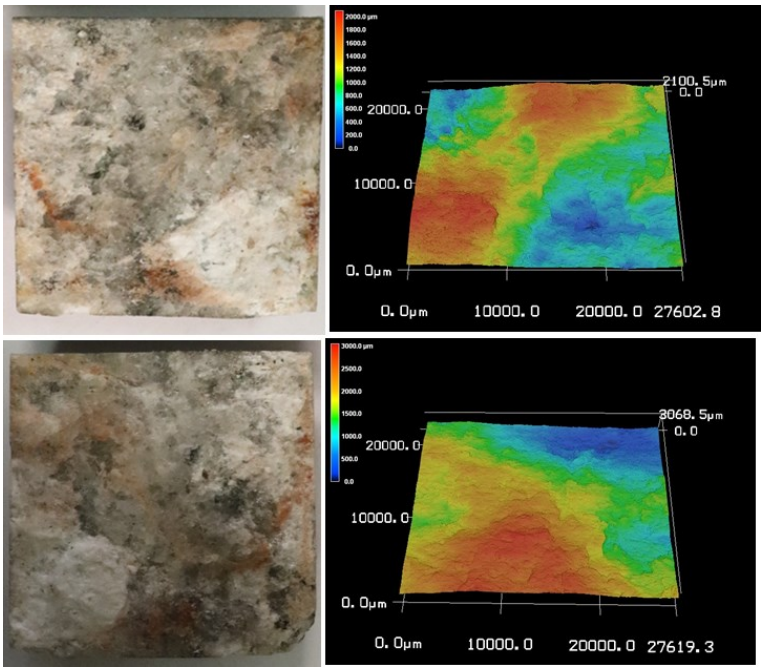

(a) FS07-01

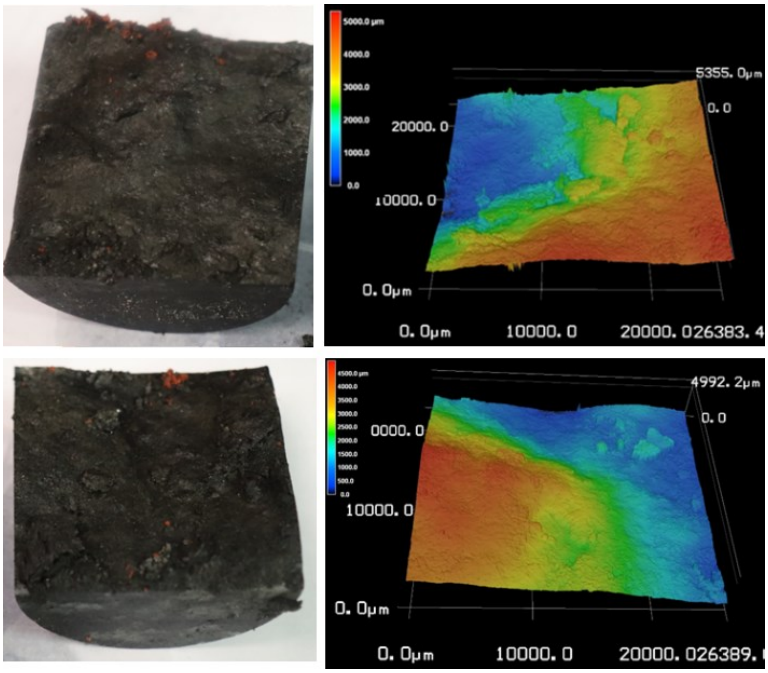

(b) FS04-01

Figure 6: Surface profilometry analysis for (a) FS07-01 (b) FS04-01. Analysis suggest shear experiments may have generated artificial slickenside fractures.

4.1 Geomechanical strength

The Mohr-Coulomb slip analysis in Figure 7 presents the measured geomechanical parameters for the two tested samples. The findings reveal that the FS07-01 sample exhibits a higher shear strength of 47.1 MPa in contrast to the FS04-01 sample, which records 30.8 MPa. This disparity is likely attributed to the foliated nature of the FS04-01 sample, suggesting a weaker response when subjected to shearing along its vulnerable foliated plane. For FS04-01, the estimated intact cohesion is 8.1 MPa with a friction angle of 32º, while for FS07-01, it is estimated to be 7.4 MPa with a friction angle of 48º. The intact cohesion values were determined with σ_{eff} considered as 36.1 MPa, assuming the Biot coefficient for this tight granite approaches zero. The friction angle values are compared to the global average of 31º (i.e., μ=0.6).

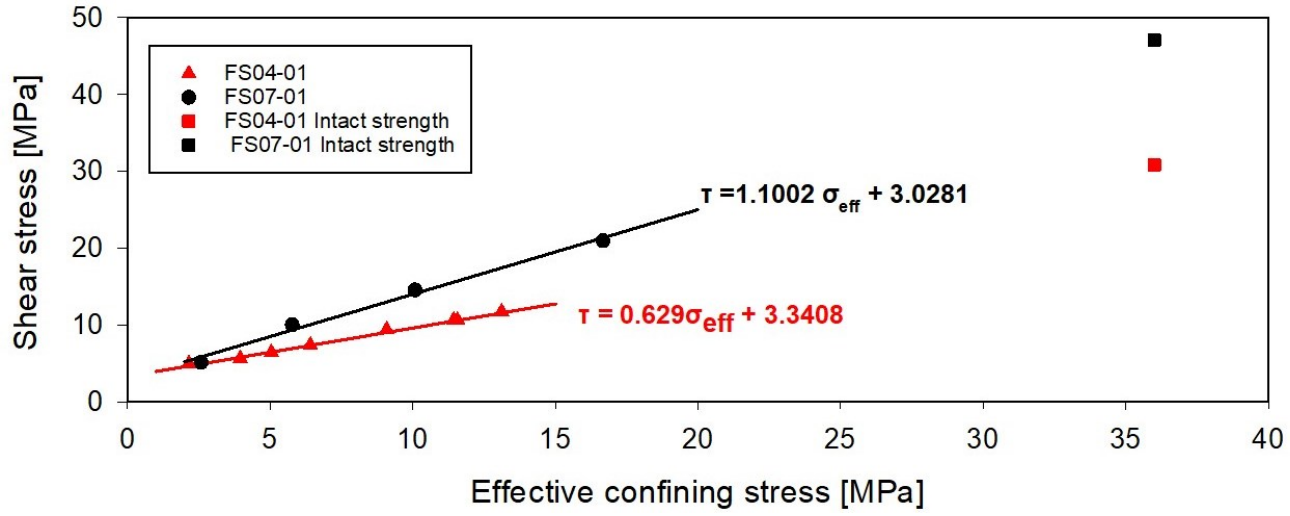

Figure 7: Measured triaxial direct-shear stresses in Mohr-Coulomb slip analysis. Fitted Mohr-Coulomb slip lines for each sample are represented by the solid lines. Additionally, the intact strength of the samples is plotted, revealing that FS04-01, characterized by strong foliation, exhibited lower strength.

4.3. Permeability and Hydraulic Aperture

Figures 8 illustrate the measured permeability and hydraulic aperture with an uncertainty estimate. At an effective confining pressure of 14.1 MPa, the intact permeability of granite samples appears to be less than or equal to 0.0001 mD. This contrasts with Mclennan (2018) prior permeability measurements on Utah FORGE Well 58-32 Cores, indicating a maximum permeability of 0.022 mD—two orders of magnitude higher than our findings. Achieving fluid circulation at economic rates in this rock poses challenges, requiring stimulation through hydro shearing or hydrofracturing (hydraulic fracturing).

After the initial shear fracturing event, there was a significant permeability increase by a factor of 10^4 or more reaching a magnitude of at least 1mD (Figures 8 upper panel). Simultaneously, the hydraulic aperture of the fracture exhibited an increase by at least a factor of 10^2, reaching a magnitude less than or equal to 0.01mm (Figure 8 lower panel). This increase persisted over time. However, subsequent shearing event (i.e. additional shear displacement) after the initial fracture event did not lead to the expected rise in hydraulic aperture and permeability typically observed at room temperature by Meng et al., (2022). After the stress cycle (Figure 5), i.e. effective confining pressure changes from of 14.1 MPa – 2 MPa – 26 MPa – 14.1 MPa, the fracture permeability experienced a reduction by a factor of 10^2. The hydraulic aperture appears to also experience a reduction to ~0.006 mm after a stress cycle. The increase in effective confining stress led to asperity compaction and breakage, resulting in fracture closure and a subsequent decrease in permeability (Fang and Wu, 2021; Zoback and Byerlee, 1975). During the cooling period, there was a significant reduction in fracture permeability by a factor of 10^2, and concurrently, the hydraulic aperture tended to diminish to approximately 0.003 mm.

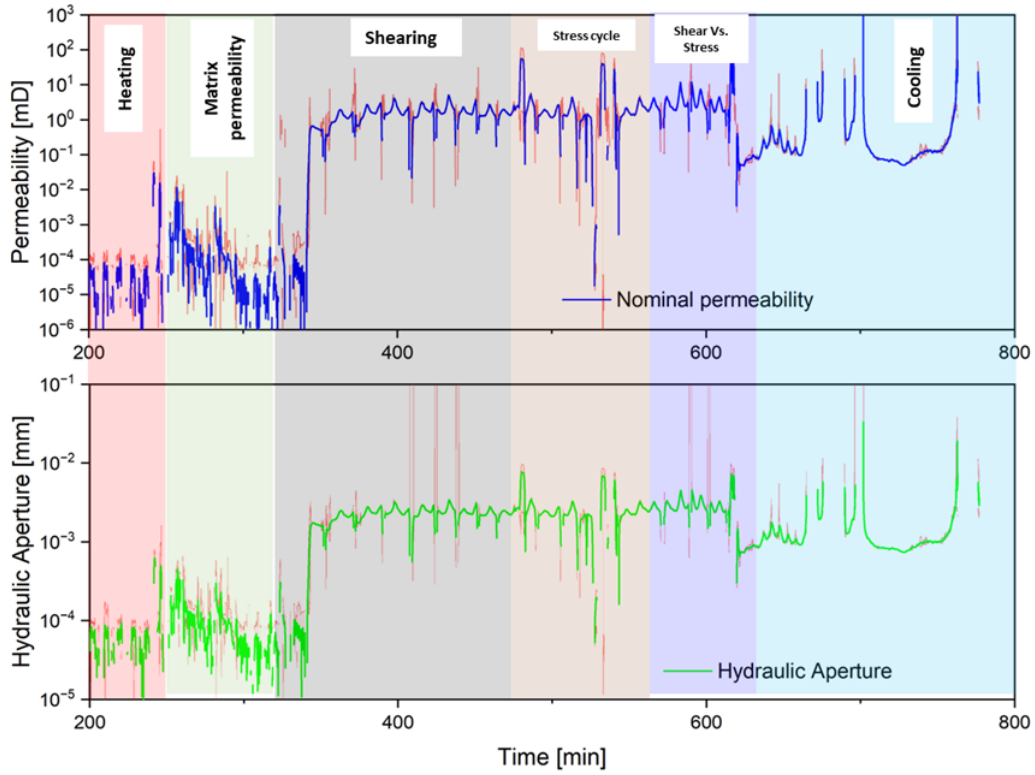

(a) FS07-01

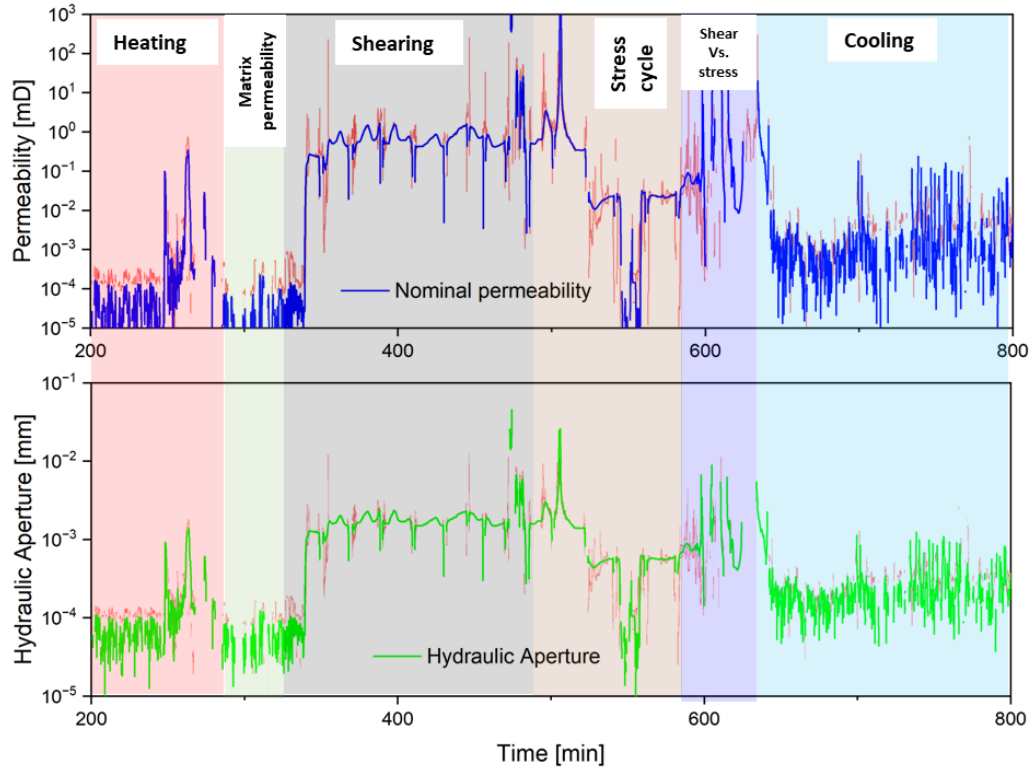

(b) FS04-01

Figure 8: Hydraulic conductivity measurements for (a) FS07-01 and (b) FS04-01. The upper panel illustrates transient permeability, with the red color indicating uncertainty in the calculated permeability. The bottom panel displays hydraulic aperture, where the red color represents uncertainty in the calculated hydraulic aperture.

4.2 Mechanical Aperture

When subjected to shear displacement and stress, the mechanical behaviour of fractures undergoes significant changes. In these experiments, we determine the variation of the mechanical aperture (b_d) across the fractured rock specimens with shear displacement, at the same confining pressure. Additionally, we investigate the variation of mechanical aperture in relation to effective confining stress. Figure 9 shows that the mechanical aperture increases with shear displacement for the tested samples. The ultra-low dilation constants of 0.069 (3.9° dilation angle) for FS07-01 and 0.063 (3.6° dilation angle) for FS04-01 contrast sharply with ambient temperature tests, which typically have nominal values closer to 0.2 (12° dilation angle). These values are notably lower than those observed in room temperature tests on similar granite samples, which typically yield an average value of 11° (Meng et al., 2022).

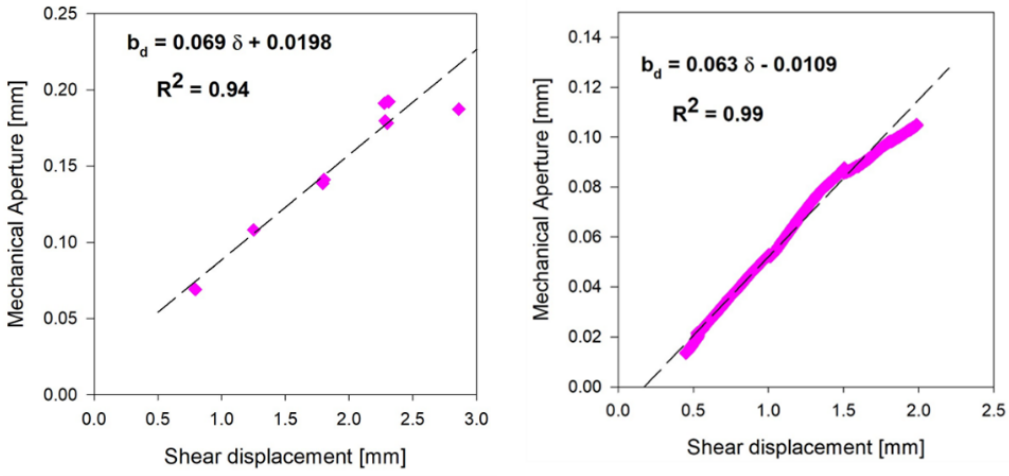

Figure 9: Mechanical aperture as a function of shear displacement at constant effective stress for (a) FS07-01 and (b) FS04-01. The arctan^{-1} of the slope of the lines indicates dilation angles of 3.9° for FS07-01 and 3.6° for FS04-01.

Figure 10 illustrates the influence of effective confining stresses on the mechanical aperture. The plot indicates a decrease in the initial mechanical aperture as the confining pressure increases, yet it does not reach zero, even at the maximum effective confining stress of 26 MPa achieved in this test. This implies the presence of voids between the fracture surfaces at high effective confining stresses. A possible explanation provided by Schrauf and Evans (1986), attributes the reduction in mechanical aperture to fracture surface deformation and damage, and possibly blockage of local channels for fluid flow as the effective confining pressure increases. Chen et al. (2000) proposed another explanation for this phenomenon, suggesting that even after the fracture surfaces close, the residual aperture distribution remains highly heterogeneous in all three dimensions due to the interaction of asperities, which maintains the fracture partially open. Our result also suggest that is dependent on stress history.

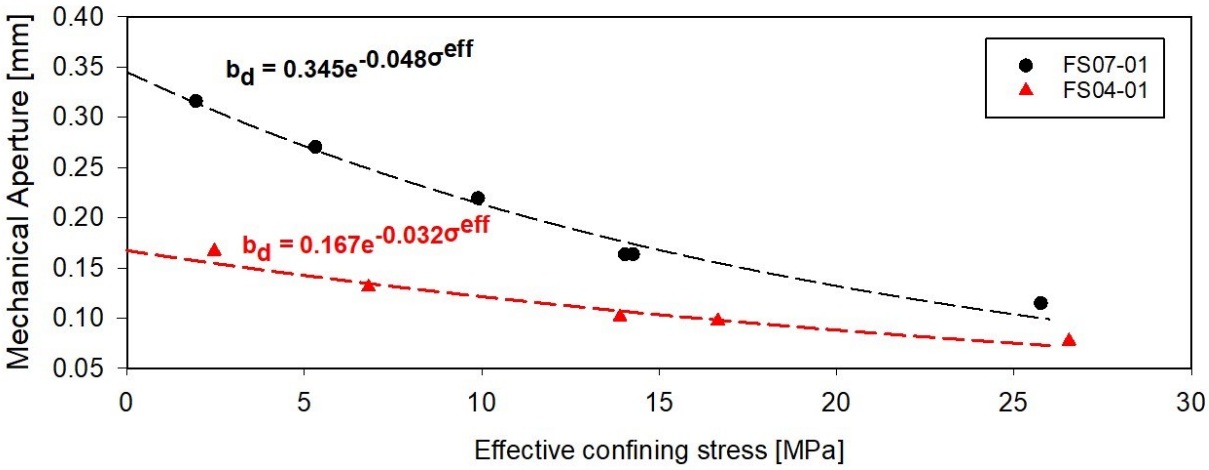

Figure 10: Relationship between mechanical aperture and effective confining stress.

4.3: Effluent water chemistry

Effluent water samples were collected during flow-through experiments to investigate changes in fluid chemistry due to mineral dissolution or interaction with the experimental apparatus. After each stepwise event, the effluent samples were collected and analyzed for cation contents using the Inductively Coupled Plasma Mass Spectrometry (ICP-MS) technique, following acidification with nitric acid. Figure 11 illustrates the temporal evolution of geochemical data for FS07-01. While effluent water samples were obtained from FS04-01, the analysis using ICP-MS to ascertain aqueous chemistry is still pending. In Figure 11, discernible common trends in effluent fluid composition are observed. Concentrations of K, Si, SiO2, Ca, and Na show an initial rise, followed by a decrease and plateau. The data supports the observation of rapid rock dissolution upon the creation of a fresh fracture surface under in-situ conditions, with this dissolution gradually decreasing over time as the flow persists. The short-lived spikes in K, Ca, and Na may be linked, at least in part, to the capture of residual geothermal brine from the rock pores or the dissolution of highly soluble phases. However, notable deviations from this trend are noted in Mg. Magnesium is traced back to the influent water, with the influent serving as a source of magnesium in the field. The complete implications of these findings are not fully understood at the time of compiling this report, necessitating further analysis.

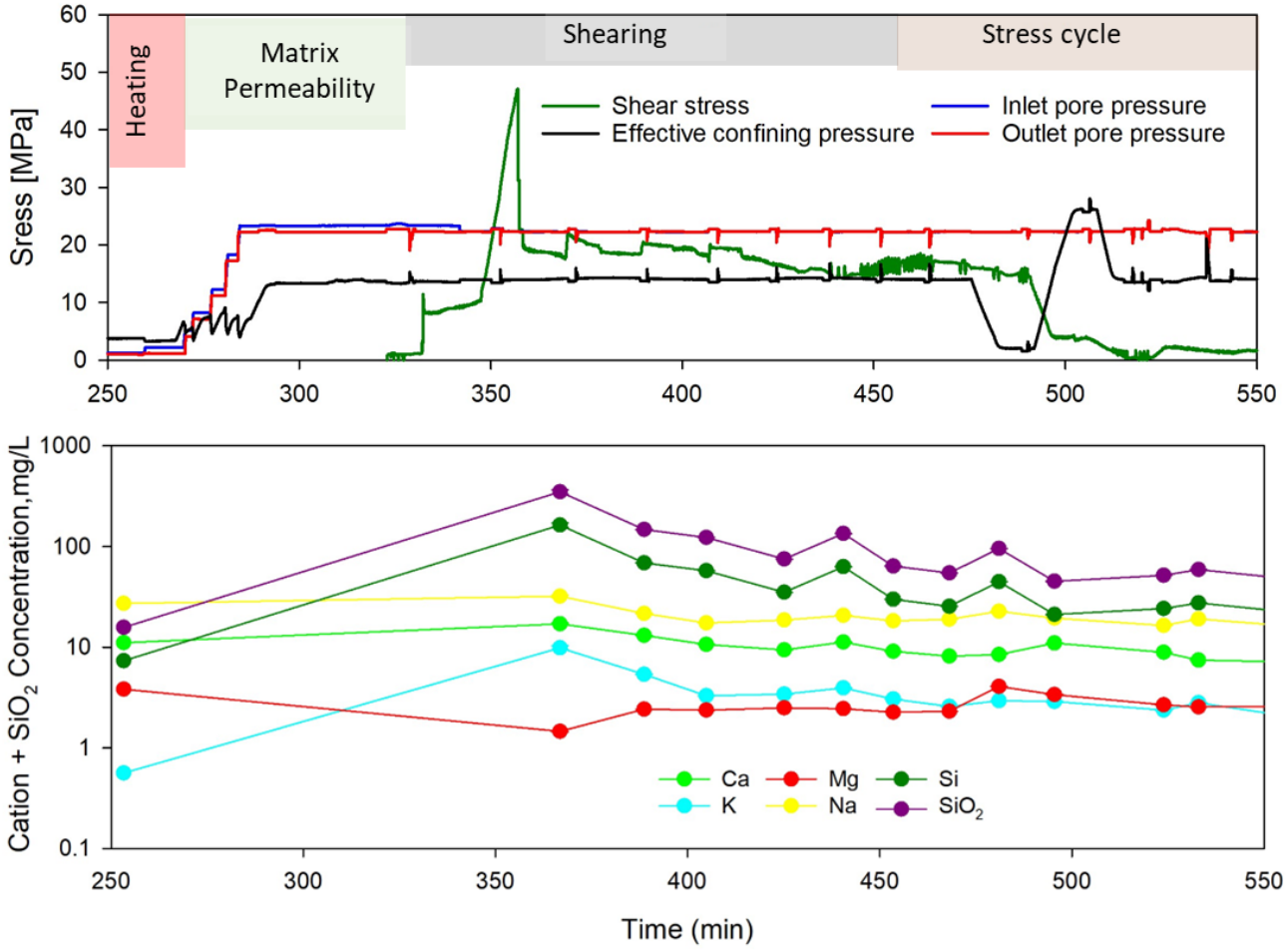

Figure 11: Geochemical data for FS07-01. The upper panels show the applied stress state, effective pressure, inlet, and outlet pore pressures as a function of time. Effluent sample collection coincides with pore pressure blips during pump disconnections and reconnections. The lower panel show the concentration of cations and SiO_2 in the effluent vs. time. Rapid dissolution of K-feldspar (e.g., $KAlSi_3O_8$) is evident after the fracture was created at 366 min.

5. DISCUSSION

The mean mechanical aperture is a measure of the void spaces or gaps between fracture surfaces, why the hydraulic aperture refers to the equivalent aperture through which fluid flow can take place within a fracture. Figure 12 illustrates the relationship between these parameters, revealing a noteworthy discrepancy—the hydraulic aperture is considerably less than the corresponding mechanical aperture. This observed trend is consistent with findings reported by others (e.g., Chen et al., 2000) This discrepancy can be attributed to the occurrence of heightened pressure losses resulting from surface roughness and tortuosity within the flow channels (Chen et al., 2000). The presence of these factors leads to an increased frictional drag on fluid flow. Particularly in scenarios where the fracture aperture is small, the influence of surface roughness and tortuosity becomes more pronounced, dominating the fluid flow behaviour. Furthermore, natural fractures, when subjected to shear motion or alteration, deviate from perfect planarity, resulting in contacts between fracture

surfaces at asperities. Under applied normal stresses, both asperities and the surrounding voids undergo deformation, leading to an increased number of asperities in contact. This process reduces the volume of voids and enhances the tortuosity of the flow channels.

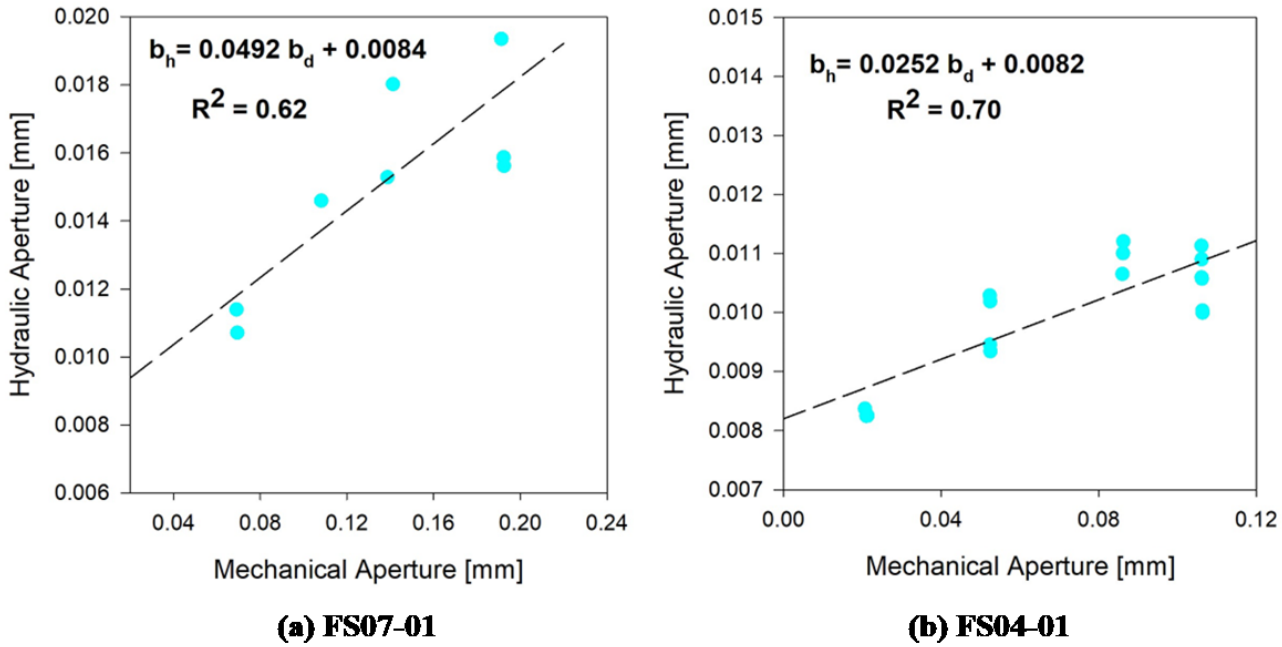

Figure 12: Relationship between mechanical aperture and hydraulic aperture for (a) FS07-01 and (b) FS04-01.

Alterations to the profile of fracture surfaces also play a crucial role in shaping the hydraulic behaviour of fractures. When fractures undergo shearing, transitioning from an initially interlocked position, there is a notable increase in the void spaces between fracture surfaces, known as the shear dilation effect. However, it's essential to recognize that the shear dilation effect can introduce certain impediments to fluid flow within fractures. Physical examination of the samples following the fracturing process revealed that soft filling materials were present between the fracture surfaces, likely formed through mineral dissolution and precipitation. Additionally, the sheared fracture surfaces appeared to be smooth resembling slickensides and felt waxy to the touch. The compaction and potential grouting of these soft materials under pressure might have hindered fluid flow through the fractures, leading to a reduction in permeability and hydraulic aperture. Furthermore, the smooth shear fracture surfaces may experience some degree of closure under confining stress, potentially diminishing the permeability and hydraulic aperture of the rock. These observations elucidate why the substantial increase in permeability and hydraulic aperture observed after the initial shear fracturing event did not lead to the expected rise.

6. CONCLUSIONS

The success of Enhanced Geothermal Systems (EGS) reservoirs relies on maintaining permeability and ensuring sufficient fluid flow through fractures in deep hot rock. As fluid is injected into the rock over time, it induces changes in pressure and temperature, leading to a feedback effect on fracture permeability through complex THMC coupling. Despite numerous coupled THMC models focusing on fracture stimulation for EGS, there is a lack of comprehensive and fully validated workflows addressing the coupled THMC processes assumed to control the long-term evolution of fracture permeability. These processes are crucial in understanding how sustained stress under hydrothermal conditions may cause changes in fracture aperture, such as compression, shear failure, mineral dissolution, and mineral precipitation. In our study, we conducted mechanical shearing and flow-through experiments on 1.5-inch diameter core samples obtained from the Utah FORGE site using a triaxial direct-shear method. The outcomes of these experiments provide essential data to validate the coupled THMC models, offering insights into permeability enhancement through shearing, shear strength, fracture mineral compositions, as well as mechanical and hydraulic aperture. From this study, several conclusions were drawn:

1. Following the initial shearing, subsequent shearing did not result in a significant increase in fracture permeability. Therefore, it should not be assumed that shear stimulation will always lead to higher hydraulic conductivity.
2. The triaxial direct shear experiments appear to have created artificial slickenside fractures associated with strong dissolution of K-feldspar and minor precipitation of magnesium salts perhaps due to the presence of these cations as contamination in the analog Milford golf course water used in the experiments.
3. Shear strength was high with an intact cohesion estimated at 7.4 to 8.1 MPa and a friction angle of 32 to 48º, compared to the global average of 31º (i.e., μ=0.6)

4. Shear stimulated hydraulic aperture appears to be quite low (~0.020 mm) perhaps due to low dilation and smooth fracture surfaces. Hydraulic aperture appears to decrease to ~0.006 mm after a stress cycle.
5. Shear dilation angle was measured at an average of 4º which is notably low compared to room temperature tests that typically yield average value of 11º.
6. Given the small dilation angles observed in our study, it appears that shear stimulation at FORGE is unlikely to significantly enhance flow.

ACKNOLEDGEMENTS

Funding for this work was provided by U.S. Department of Energy's (DOE), Energy Efficiency and Renewable Energy (EERE) Geothermal Technologies Office (GTO) Frontier Observatory for Research in Geothermal Energy (FORGE) under grant DE-EE0007080 with Lawrence Livermore National Laboratory

REFERENCES

Allis, Rick, Joe Moore, Nick Davatzes, Mark Gwynn, Christian Hardwick, Stefan Kirby, John McLennan, et al. "EGS Concept Testing and Development at the Milford, Utah Forge Site." Paper presented at the Proceedings, 2016.

Augustine, Chad. Update to Enhanced Geothermal System Resource Potential Estimate. National Renewable Energy Lab.(NREL), Golden, CO (United States) (2016).

Chen, Z., S. P. Narayan, Z. Yang, and S. S. Rahman. "An Experimental Investigation of Hydraulic Behaviour of Fractures and Joints in Granitic Rock." International Journal of Rock Mechanics and Mining Sciences 37, no. 7 (2000/10/01/ 2000): 1061-71.

D4543-08, ASTM. Standard Practices for Preparing Rock Core as Cylindrical Test Specimens and Verifying Conformance to Dimensional and Shape Tolerances. ASTM International, 2008.

Davatzes, Nicholas c., and Stephen H. Hickman. "The Feedback between Stress, Faulting, and Fluid Flow : Lessons from the Coso Geothermal Field , Ca , USA." 2009.

Dobson, Patrick F., Timothy J. Kneafsey, Seiji Nakagawa, Eric L. Sonnenthal, Marco Voltolini, J. Torquil Smith, and Sharon E. Borglin. "Fracture Sustainability in Enhanced Geothermal Systems: Experimental and Modeling Constraints." Journal of Energy Resources Technology 143, no. 10 (2021).

Fang, Zhou, and Wei Wu. "Laboratory Friction-Permeability Response of Rock Fractures: A Review and New Insights." Geomechanics and Geophysics for Geo-Energy and Geo-Resources 8, no. 1 (2021/12/03 2021): 15

Frash, L. P., J. W. Carey, Z. Lei, E. Rougier, T. Ickes, and H. S. Viswanathan. "High-Stress Triaxial Direct-Shear Fracturing of Utica Shale and in Situ X-Ray Microtomography with Permeability Measurement." Article. Journal of Geophysical Research: Solid Earth 121, no. 7 (2016): 5493-508.

Frash, Luke P., J. William Carey, Timothy Ickes, and Hari S. Viswanathan. "Caprock Integrity Susceptibility to Permeable Fracture Creation." International Journal of Greenhouse Gas Control 64 (2017/09/01/ 2017): 60-72.

Frash, Luke P., J. William Carey, and Nathan J Welch. "EGS Collab Experiment 1 Geomechanical and Hydrological Properties by Triaxial Direct Shear." Paper presented at the 44th workshop on geothermal reservoir engineering, 2019.

Frash, Luke P., J. William Carey, and Nathan J. Welch. "Scalable En Echelon Shear-Fracture Aperture-Roughness Mechanism: Theory, Validation, and Implications." Journal of Geophysical Research: Solid Earth 124, no. 1 (2019): 957-77.

Huo, Da, and Sally M. Benson. "Experimental Investigation of Stress-Dependency of Relative Permeability in Rock Fractures." Transport in Porous Media 113, no. 3 (2016/07/01 2016): 567-90

Jones, Clay G, Joseph N Moore, and Stuart F Simmons. "Lithology and Mineralogy of the Utah FORGE EGS Reservoir: Beaver County, Utah." GRC Trans 42 (2018).

Li, Wenfeng, Luke P. Frash, Nathan J. Welch, J. William Carey, Meng Meng, and Marcus Wigand. "Stress-Dependent Fracture Permeability Measurements and Implications for Shale Gas Production." Fuel 290 (2021/04/15/ 2021): 119984.

Li, Wenfeng, Chelsea W Neil, J William Carey, Meng Meng, Luke P Frash, and Philip H Stauffer. "Hydromechanical Characterization of Gas Transport Amidst Uncertainty for Underground Nuclear Explosion Detection." Journal of Rock Mechanics and Geotechnical Engineering (2023).

McKittrick, Alexis, Leslie Abrahams, Christopher Clavin, Robert Rozansky, and Daniel Bernstein. Frontier Observatory for Research in Geothermal Energy: A Roadmap. Institute for Defense Analyses., 2019.

McLennan, John. "Utah Forge: Well 58-32 Core Analyses." Energy and Geoscience Institute at the University of Utah, 2018/05/30 2018.

Meng, Meng, Luke P. Frash, Wenfeng Li, Nathan J. Welch, and J. William Carey " Measurement of Geomechanical and Hydrological Properties of EGS-Collab Geothermal Rocks." Paper presented at the 55th US Rock Mechanics/Geomechanics Symposium, 2021.

Meng, Meng, Luke P. Frash, Wenfeng Li, Nathan J. Welch, J. William Carey, Joseph Morris, Ghanashyam Neupane, Craig Ulrich, and Timothy Kneafsey. "Hydro-Mechanical Measurements of Sheared Crystalline Rock Fractures with Applications for EGS-Collab Experiments 1 and 2." Journal of Geophysical Research: Solid Earth 127, no. 2 (2022): e2021JB023000.

Milsch, Harald, Hannes Hofmann, and Guido Blöcher. "An Experimental and Numerical Evaluation of Continuous Fracture Permeability Measurements During Effective Pressure Cycles." International Journal of Rock Mechanics and Mining Sciences 89 (2016): 109-15.

Moore, Joseph, John McLennan, Rick Allis, Kristine Pankow, Stuart Simmons, Robert Podgorney, Philip Wannamaker, et al. "The Utah Frontier Observatory for Research in Geothermal Energy (Forge): An International Laboratory for Enhanced Geothermal System Technology Development." Paper presented at the 44th Workshop on Geothermal Reservoir Engineering, 2019.

Morrow, C. A., D. E. Moore, and D. A. Lockner. "Permeability Reduction in Granite under Hydrothermal Conditions." Journal of Geophysical Research: Solid Earth 106, no. B12 (2001): 30551-60.

Nielson, Dennis L, STANLEY H EVANS JR, and Bruce S Sibbett. "Magmatic, Structural, and Hydrothermal Evolution of the Mineral Mountains Intrusive Complex, Utah." Geological Society of America Bulletin 97, no. 6 (1986): 765-77.

Sanyal, Subir K, and Steven J Butler. "An Analysis of Power Generation Prospects from Enhanced Geothermal Systems." Geothermal Resources Council Transactions 29 (2005): 131-8.

Schrauf, T. W., and D. D. Evans. "Laboratory Studies of Gas Flow through a Single Natural Fracture." Water Resources Research 22, no. 7 (1986): 1038-50.

Tester, Jefferson W, Brian J Anderson, Anthony S Batchelor, David D Blackwell, Ronald DiPippo, Elisabeth M Drake, John Garnish, et al. "Impact of Enhanced Geothermal Systems on Us Energy Supply in the Twenty-First Century." Philosophical Transactions of the Royal Society A: Mathematical, Physical and Engineering Sciences 365, no. 1853 (2007): 1057-94.

Vogler, D., R. R. Settgast, C. Annavarapu, C. Madonna, P. Bayer, and F. Amann. "Experiments and Simulations of Fully Hydro-Mechanically Coupled Response of Rough Fractures Exposed to High-Pressure Fluid Injection." Journal of Geophysical Research: Solid Earth 123, no. 2 (2018): 1186-200.

Welch, Nathan J, J William Carey, Luke P Frash, Jeffrey D Hyman, Wes Hicks, Meng Meng, Wenfeng Li, and Anne H Menefee. "Effect of Shear Displacement and Stress Changes on Fracture Hydraulic Aperture and Flow Anisotropy." Transport in Porous Media (2021): 1-31.

Witherspoon, P. A., J. S. Y. Wang, K. Iwai, and J. E. Gale. "Validity of Cubic Law for Fluid Flow in a Deformable Rock Fracture." Water Resources Research 16, no. 6 (1980): 1016-24.

Xing, P., McLennan, J., Moore, J. “In-Situ Stress Measurements at the Utah Frontier Observatory for Research in Geothermal Energy (FORGE) Site”. Energies. 2020 Nov 9;13(21):5842

Yasuhara, Hideaki, Derek Elsworth, and Amir Polak. "Evolution of Permeability in a Natural Fracture: Significant Role of Pressure Solution." Journal of Geophysical Research: Solid Earth 109, no. B3 (2004).

Zimmerman, Robert W, and Gudmundur S Bodvarsson. "Hydraulic Conductivity of Rock Fractures." Transport in porous media 23 (1996): 1-30.

Zoback, Mark D, and JD Byerlee. "Permeability and Effective Stress." AAPG Bulletin 59, no. 1 (1975): 154-58.